*Korean J. of Chem. Eng.*, **11**(1), 14-24 (1994)

# EFFECT OF CATALYST PORE STRUCTURE ON EFFECTIVE DIFFUSIVITY

**Young-Woo Rhee* and James A. Guin**

*Korea Institute of Energy Research, 71-2 Jang-dong, Yoosung-gu, Taejon, Korea
Department of Chemical Engineering, Auburn University, Auburn, AL 36849, U.S.A.
*(Received 9 January 1993 • accepted 7 October 1993)*

**Abstract**—The effective diffusivity of the catalyst was experimentally measured in both octane-decane and polystyrene-chloroform systems for comparison with effects identified in the coal liquefaction model work. The diffusivity data were in good agreement with the theoretical solution and their reproducibility was satisfactory. In both experimental systems, the effective diffusivity was strongly dependent upon the ratio of diffusing species to catalyst pore size. When the steric exclusion-hydrodynamic drag theory was applied, the tortuosity significantly varied with the ratio of diffusing molecule to catalyst pore size. Using the diffusivity data of unimodal catalysts, an empirical equation relating the size ratio to the restrictive factor was derived to evaluate the diffusivity data of bimodal catalysts.

## INTRODUCTION

As elucidated in the previous paper [1], the effective diffusivity is one of the main factors having significant effects on the catalyst activity. The model demonstrated that the catalyst with larger pores had higher effective diffusivity and, therefore, gave higher activity unless the surface area was extremely small. This effect, identified in the previous model work [1], was experimentally evaluated by measuring the effective diffusivity in two different diffusion systems, i.e. octane in decane and polystyrene in chloroform.

The two diffusion systems were chosen in order to obtain the tortuosity. As shown in the previous paper [1], the effective diffusivity is apparently a function of the ratio of reactant molecule size to pore size, $\lambda$. The tortuosity $\tau$ may be calculated from the experimental values of the effective diffusivity, porosity, and molecular diffusivity, since the size of octane is much smaller than the pore size in the octane-decane system. In the polystyrene-chloroform diffusion system, the size of polystyrene is comparable to the pore size, thus making the effect of $\lambda$ on the effective diffusivity more significant. This effect is expressed in terms of $F(\lambda)$ and is shown in Eq. (1).

$$D_e = \frac{D_m}{\tau} \Sigma \varepsilon_i F(\lambda_i) \tag{1}$$

If the tortuosity obtained in the octane-decane system is used to calculate $F(\lambda)$, then the effect of the pore-to-reactant molecule size ratio on the tortuosity may be obtained by comparing this $F(\lambda)$ with the $F(\lambda)$ calculated using Eq. (1). The evidence for the dependence of $\lambda$ on the tortuosity has been reported in the literature [2].

In this research the ratio of pore to molecule size was systematically changed by selecting polystyrene of different sizes for a catalyst. The diffusion apparatus developed by Tsai [3] was used for these experiments. The effective diffusivity values were obtained from a least square fit of the experimental data to the analytical solution curve. From these experiments, the degree of pore connectivity, which was assumed to be perfect in the model, was evaluated.

## THEORY

The governing equation describing the diffusion of a solute in the porous pellet is as follows [4]:

$$\rho_r \frac{\partial q}{\partial t} + \varepsilon_a \frac{\partial C}{\partial t} = D_e \nabla^2 C \tag{2}$$

Here, the adsorption by the solute, represented in the first term of Eq. (2), is assumed to be negligible. There-

*The author to whom correspondences should be addressed.

fore,

$$\varepsilon_a \frac{\partial C}{\partial t} = D_e \nabla^2 C \tag{3}$$

Actually, this assumption will be proven to hold for the diffusion experiments outlined in subsequent sections of this paper. The boundary conditions for Eq. (3) are:

$$\text{B.C. 1: at } r = d/2,\ C = C_b \tag{4}$$

$$\text{B.C. 2: at } r = 0,\ \partial C/\partial r = 0 \tag{5}$$

A material balance on the solute in the finite diffusion bath without any external mass transfer resistance will be

$$V_b \frac{dC_b}{dt} = \int_s N_A dS = -\int_s (D_e \nabla C \cdot n) dS \tag{6}$$

Eq. (6) can be rewritten as Eq. (7) using the divergence theorem.

$$V_b \frac{dC_b}{dt} = \int_v \frac{\partial C}{\partial t} dV_{pore} \tag{7}$$

By substituting the relationship $V_{pore} = \varepsilon_a V_{tp}$ into Eq. (7),

$$V_b \frac{dC_b}{dt} = \varepsilon_a \int_v \frac{\partial C}{\partial t} dV_{tp} \tag{8}$$

Here, C is a function of time and local position inside the pellet. The initial conditions are:

$$\text{I.C. 1: at } t = 0,\ C = C_i \tag{9}$$

$$\text{I.C. 2: at } t = 0,\ C_b = C_{bi} \tag{10}$$

In order to simplify the problem, the following dimensionless variables were defined:

$$C^* = \frac{C - C_i}{C_{bi} - C_i} \tag{11}$$

$$C_b^* = \frac{C_b - C_i}{C_{bi} - C_i} \tag{12}$$

$$\theta = \frac{D_e t}{\varepsilon_a (d/2)^2} = \frac{D_e' t}{(d/2)^2} \tag{13}$$

$$\xi = \frac{V_b}{V_{tp}} \tag{14}$$

$$r^* = \frac{r}{d/2} \tag{15}$$

Therefore Eqs. (3)-(5) and (8)-(10) can be rewritten as follows:

$$\frac{\partial C^*}{\partial \theta} = \nabla^2 C^* \tag{16}$$

$$\text{B.C. 1: at } r^* = 1,\ C^* = C_b^* \tag{17}$$

$$\text{B.C. 2: at } r^* = 0,\ \partial C^*/\partial r^* = 0 \tag{18}$$

$$\frac{dC_b^*}{d\theta} = -\frac{1}{\alpha} \int \frac{\partial C^*}{\partial \theta} d\xi \tag{19}$$

$$\text{I.C. 1: at } \theta = 0,\ C^* = 0 \tag{20}$$

$$\text{I.C. 2: at } \theta = 0,\ C_b^* = 1 \tag{21}$$

where

$$\alpha = \frac{V_b}{\varepsilon_a V_{tp}} = \frac{V_b}{V_{pore}} \tag{22}$$

In the diffusion experiments performed here, the $\alpha$ value is large (>200) enough for the right-hand side of Eq. (19) to be neglected. In other words, the quasi-steady state can be assumed for the solute concentration in the bulk phase $C_b$. The initial distribution of the solute inside the pellet is assumed uniform. Then, an analytical solution for Eqs. (16) and (19) exists as follows [5]:

$$\frac{M_t}{M_\infty} = \left(\frac{M_t}{M_\infty}\right)_1 + \left(\frac{M_t}{M_\infty}\right)_2 \left[1 - \left(\frac{M_t}{M_\infty}\right)_1\right] \tag{23}$$

where $M_t/M_\infty$ = fractional approach to the equilibrium

$M_t$ = total amount of the solute diffusing out of the pellets till time t

$M_\infty = M_t$ at time $t = \infty$

Subscript 1 is used for the slab geometry and subscript 2 for the cylindrical geometry.

Because the pellets used in the diffusion experiments have a diameter-to-length ratio of one, $(M_t/M_\infty)_1$ and $(M_t/M_\infty)_2$, in Eq. (23), can be expressed as follows [6]:

$$\left(\frac{M_t}{M_\infty}\right)_1 = 1 - \sum_{n=0}^{\infty} \frac{8}{(2n+1)^2 \pi^2} \exp[-(n+1/2)^2 \pi^2 \theta] \tag{24}$$

$$\left(\frac{M_t}{M_\infty}\right)_2 = 1 - \sum_{n=1}^{\infty} \frac{4}{\beta_n^2} \exp(-\beta_n^2 \theta) \tag{25}$$

where $\beta_n$ is the root in the Bessel function of the first kind of order zero. Their values are listed in Table 1 up to n=20 [7].

In order to investigate the effect of on the analytical solution curve, the $\alpha$ value was selected as 9 (this value is equivalent to 10% solute uptake by the pellets). Diffusion from a stirred solution of limited volume is well discussed in the literature and Eqs. (24)

**Table 1. Roots in Eqs. (23)-(29)**

| n | $\beta_n$ | $X_n$ | $Y_n$ |
|---|---|---|---|
| 1 | 2.40483 | 1.6385 | 2.4922 |
| 2 | 5.52008 | 4.7359 | 5.5599 |
| 3 | 8.65373 | 7.8681 | 8.6793 |
| 4 | 11.79153 | 11.0057 | 11.8103 |
| 5 | 14.93092 | 14.1451 | 14.9458 |
| 6 | 18.07106 | 17.2852 | 18.0833 |
| 7 | 21.21164 | 20.4258 | 21.2221 |
| 8 | 24.35247 | 23.5667 | 24.3616 |
| 9 | 27.49348 | 26.7077 | 27.5015 |
| 10 | 30.63461 | 29.8489 | 30.6418 |
| 11 | 33.77582 | 32.9901 | 33.7824 |
| 12 | 36.91710 | 36.1314 | 36.9231 |
| 13 | 40.05843 | 39.2728 | 40.0639 |
| 14 | 43.19979 | 42.4141 | 43.2049 |
| 15 | 46.34119 | 45.5555 | 46.3460 |
| 16 | 49.48261 | 48.6970 | 49.4871 |
| 17 | 52.62405 | 51.8384 | 52.6283 |
| 18 | 55.76551 | 54.9799 | 55.7695 |
| 19 | 58.90698 | 58.1214 | 58.9107 |
| 20 | 62.04847 | 61.2629 | 62.0520 |

and (25) can be replaced with the following Eqs. [8]:

$$\left(\frac{M_t}{M_\infty}\right)_1 = 1 - \sum_{n=1}^{\infty} \frac{2\alpha(1+\alpha)}{1+\alpha+\alpha^2 X_n^2}\exp(-X_n^2\theta) \tag{26}$$

where $\tan X_n = -\alpha X_n$ (27)

$$\left(\frac{M_t}{M_\infty}\right)_2 = 1 - \sum_{n=1}^{\infty} \frac{4\alpha(1+\alpha)}{4+4\alpha+\alpha^2 Y_n^2}\exp(-Y_n^2\theta) \tag{28}$$

where $\alpha Y_n J_0(Y_n) + 2J_1(Y_n) = 0$ (29)

The values for $X_n$ and $Y_n$ are listed in Table 1 [6].

As can be seen in Fig. 1 where $M_t/M_\infty$ is plotted against $\theta^{1/2}$, the effect of $\alpha$ on the solution curve is not great. This result ensures that a large amount of sample can be taken out of the diffusion bath for analysis. The insensitivity of $\alpha$ is desirable especially for a UV analysis, where several milliliters of sample is withdrawn each time.

In the octane-decane diffusion experiment, $M_t/M_\infty$ will be same as $C_b/C_{b\infty}$ because only a small amount of sample is withdrawn each time for analysis using GC. However, in the case of the polystyrene-chloroform diffusion experiment, $M_t/M_\infty$ cannot be replaced with $C_b/C_{b\infty}$ because of the bulk volume change due to the relatively large amount of samples taken from the diffusion bath. Therefore, a careful record of the amount of the solute and solvent withdrawn from the bath is needed in order to obtain accurate $M_t$ and $M_\infty$ values.

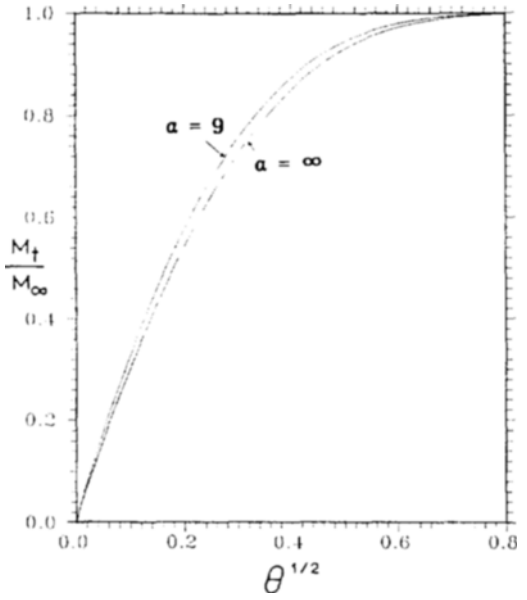


**Fig. 1. Effect of $\alpha$ in Eq. (22) on the analytical solution curve of $M_t/M_\infty$ vs. $\theta^{1/2}$.**

**Table 2. Catalyst properties for calculating effective diffusivity**

| Catalyst name | Porosity ($\varepsilon$) | Pellet length(d) (cm) | Apparent density($\rho_s$) (g/cc) |
|---|---|---|---|
| G | 0.58 | 0.449 | 1.47 |
| I | 0.62 | 0.448 | 1.49 |
| C | 0.52 | 0.390 | 1.50 |
| D | 0.43 | 0.336 | 2.27 |
| J | 0.61 | 0.454 | 1.29 |
| K | 0.72 | 0.484 | 0.90 |

## EXPERIMENTAL

### 1. Material

4.8 mm laboratory-prepared supports and catalysts were used in the diffusion experiments. The catalyst properties needed for the calculation of effective diffusivity are listed in Table 2.

The following chemicals were used as received: decane (Fisher, certified), octane (Fisher, reagent grade), toluene (Fisher, certified A.C.S.), and chloroform (Fisher, 99 mol%). The physical properties of polystyrenes provided by the manufacturer (Pressure Chemical, Pittsburgh) are given in Table 3.

### 2. Equipment

A glass diffusion cell, shown in Fig. 2, was used

**Table 3. Physical properties of polystyrene**

| Batch number | 31011 | 50822 | 40717 | 50211 | 40627 | 31116 | 50123 |
|---|---|---|---|---|---|---|---|
| By size exclusion chromatography: | | | | | | | |
| $M_w$ | 645 | 794 | 1,011 | 1,415 | 1,397 | 1,672 | 2,423 |
| $M_n$ | 568 | 700 | 906 | 1,300 | 1,306 | 1,574 | 2,276 |
| $M_p$ | 581 | 761 | 1,036 | 1,356 | 1,412 | 1,681 | 2,450 |
| By intrinsic viscosity: | | | | | | | |
| $M_v$ | – | 687 | – | 1,412 | – | – | 2,425 |
| By nuclear magnetic viscosity: | | | | | | | |
| $M_n$ | 578 | 764 | 896 | – | – | 1,523 | – |
| Diameter[a] (angstroms) | 12.0 | 13.5 | 15.7 | 19.3 | 19.4 | 21.6 | 26.8 |

a: Calculated based on $M_n$ using the following equation; $\langle R^2 \rangle^{1/2} = 0.150\ M^{0.581}$

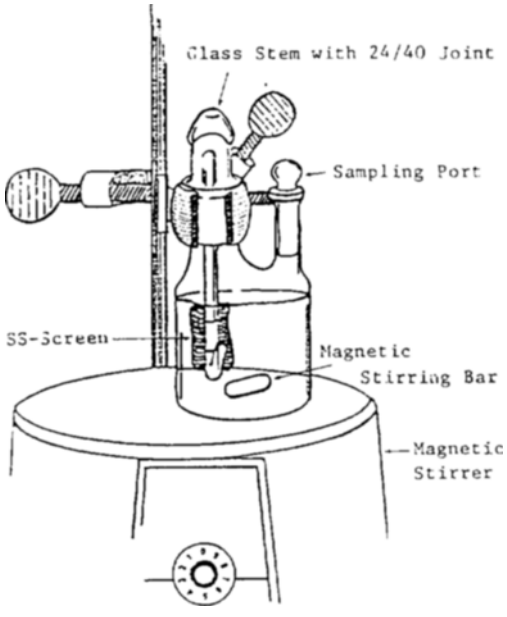


**Fig. 2. Schematic diagram of diffusion cell.**

for the diffusion experiments. The volume of the diffusion cell is about 180 cc. In order to remove any external mass transfer resistance, a magnetic stirrer was used with a stirring bar. A cylindrical stainless steel screen was designed to hold the pellets and prevent them from being crushed by the stirring bar.

Prior to making a diffusion run, the pellets were equilibrated in a dense solute solution of known concentration. For this soaking step, a 250 mL bottom flat flask with a 24/40 joint was used in the octane-decane system; a 20 mL bottom flat cylinder with a 24/40 joint was designed and used in the polystyrene-chloroform system. Because of the high cost of polystyrenes an effort was made to minimize the amount of polystyrenes by reducing the volume of the glass cylinder. As shown in Fig. 2, a glass stem was designed to hold a cylindrical stainless steel screen. It has a 24/40 joint on the top and a hook at the bottom.

A gas chromatograph (Varian model 3700) equipped with a J & W DB-5 capillary column was used to analyze the composition of octane. Toluene was used as an internal standard. The concentration of polystyrene was analyzed using a UV spectrophotometer (Gilford model 250).

### 3. Procedure

In order to use the mathematical model developed in the previous section, pellets with a length to diameter ratio of 1 were prepared. Approximately one gram of the pellets were kept in an oven at 100C for one day to remove moisture. The dried pellets were placed in the stainless steel screen and equilibrated in a 10% octane in decane solution for one day (or for one week in the case of a concentrated polystyrene-chloroform solution).

Prior to starting a run the stem containing the screen was dipped in a pure decane solution (or pure chloroform solution for the polystyrene-chloroform system) to rinse out any extraneous solute and then transferred into the bath filled with about 150 mL of pure decane (or about 170 mL of pure chloroform for the polystyrene-chloroform system). This operation was rapidly performed to avoid any elution of solution from the pellets. The large volume of decane (or chloroform) in the bath ensured that the $\alpha$ value in Eq. (22) was greater than 200.

To eliminate external mass transfer resistance, the system was agitated at a speed of about 1000 rpm. During the diffusion run several 0.5 mL samples (or 2 mL samples for the polystyrene-chloroform system) were withdrawn for analysis. The equilibrium concentration of the octane-decane system was attained in 24 hours. The polystyrene-chloroform system reached equilibrium in about 7 to 10 days.

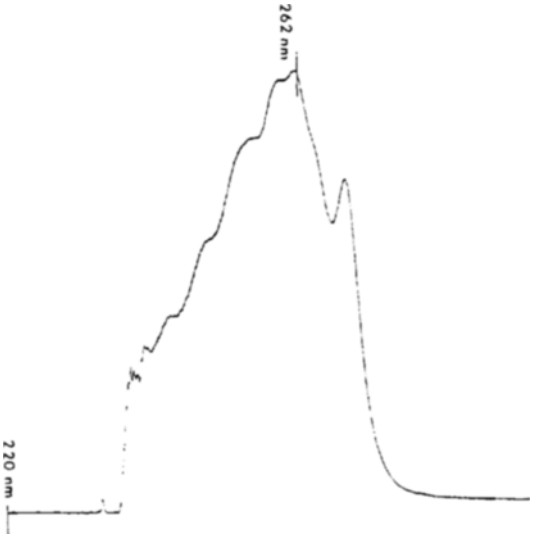


**Fig. 3. UV scanning of the polystyrene-chloroform solution.**

Fig. 3 shows the sensitivity of the UV range for the polystyrene-chloroform solution. The maximum absorbance was obtained at 262 nm. As expected the calibration curves were insensitive to the molecular weight of polystyrene.

The pellets used in the diffusion experiments were regenerated, for use in subsequent experiments, in a tube furnace provided with air flow and maintained at 450℃ for about 5 days. Adsorption experiments were performed to ensure that the adsorption term in Eq. (2) is negligible. In the polystyrene-chloroform diffusion experiment, the oven dried pellets were equilibrated with a dilute polystyrene-chloroform solution for several days and the variations in UV readings before and after were measured.

## RESULTS AND DISCUSSION

### 1. Computer Simulation

The effective diffusivity was simulated to minimize the deviation between the theoretical and experimental $M_t/M_\infty$ data as shown in Fig. 4. Eqs. (23)-(25) were used to simulate the experimental $M_t/M_\infty$ data by assuming a series of different $D_e'$ values. Finally, plots of experimental $M_t/M_\infty$ data vs. $\theta^{1/2}$ were prepared for comparison with the theoretical $M_t/M_\infty$ vs. $Q^{1/2}$ curve.

### 2. Octane-Decane System

In order to investigate the possibility of adsorption of octane or decane, catalyst K pellets were placed

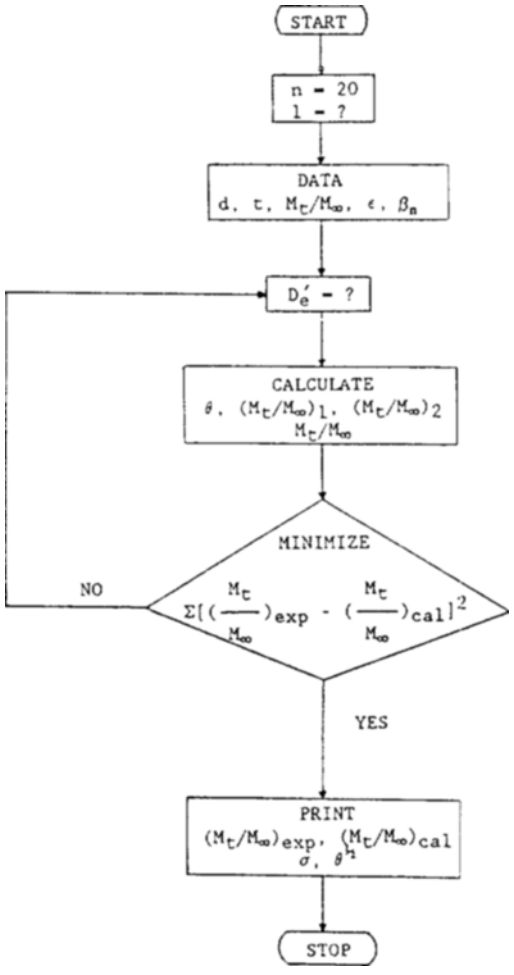


**Fig. 4. Algorithm of the computer simulation for calculating effective diffusivity.**

in closed vials with about 0.04 wt% octane in decane solution and equilibrated overnight. No change in the solution composition was observed, which means that no selective adsorption occurs onto the catalyst pellets by octane or decane.

The effect of agitation speed on the fractional approach of the octane concentration to equilibrium is shown in Fig. 5. The agitation speed of 1000 rpm seemed high enough to remove any possible mass transfer resistance at the outside of the catalyst pellets. The experimental concentrations in the bulk fluid after approximately 24 hours agreed well with the theoretical values as shown in Table 4. A little deviation between the experimental and theoretical values may come from the washing process or use of different porosity values. The magnitude of this deviation is

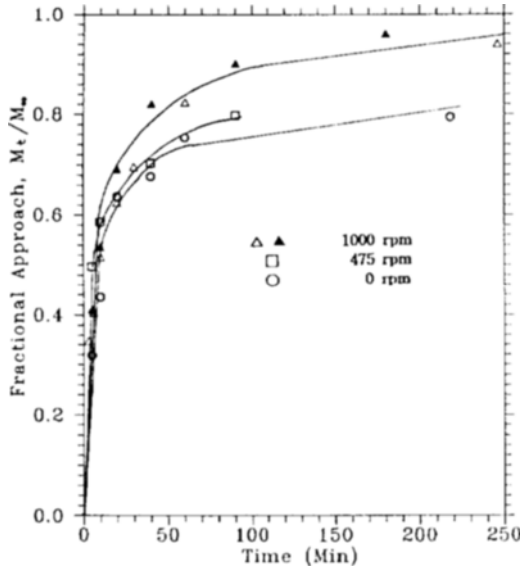


**Fig. 5. Effect of agitation speed on fractional approach to the equilibrium using catalyst G.**

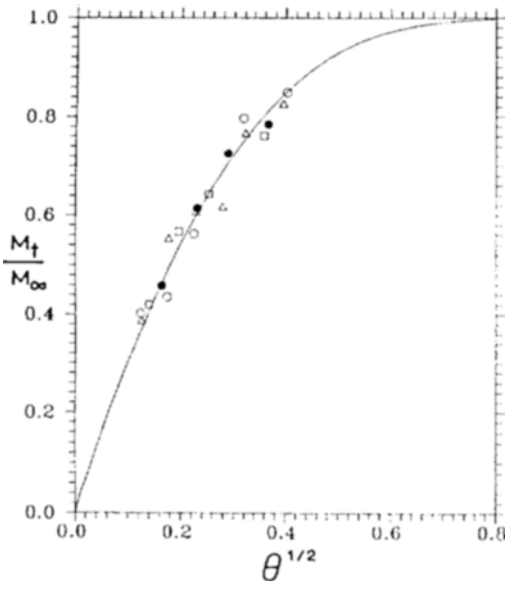


**Fig. 6. Comparison of theoretical and experimental diffusion data for catalyst K in octane-decane system.**

**Table 4. Comparison of theoretical and experimental solute concentration in the bath after a long time in octane-decane diffusion experiments**

| Catalyst | Run number | $C_{b_\infty}$ theoretical wt% | $C_{b_\infty}$ experimental wt% |
|---|---|---|---|
| G | 1 | 0.0263 | 0.0245 |
| | 2 | 0.0266 | 0.0256 |
| | 3 | 0.0250 | 0.0236 |
| I | 4 | 0.0258 | 0.0219 |
| | 5 | 0.0275 | 0.0269 |
| C | 6 | 0.0218 | 0.0235 |
| | 7 | 0.0234 | 0.0235 |
| D | 8 | 0.0131 | 0.0125 |
| | 9 | 0.0123 | 0.0126 |
| J | 10 | 0.0301 | 0.0290 |
| | 11 | 0.0300 | 0.0314 |
| K | 12 | 0.0425 | 0.0368 |
| | 13 | 0.0504 | 0.0413 |
| | 14 | 0.0503 | 0.0463 |
| | 15 | 0.0530 | 0.0443 |

similar to the data reported in the literature [3]. A good agreement between theoretical and experimental $C_{b_\infty}$ implies that all catalyst pores were filled up with the solution during the soaking procedure. In the case of catalyst K, around 14% deviation was consistently observed, which suggests that the porosity of catalyst K may have been overestimated. In other words, the true value of porosity may be smaller than that listed in Table 2.

The diffusivity data are in good agreement with the theoretical solution as typically shown in Fig. 6. Effective diffusivity values are listed in Table 5. The reproducibility was satisfactory except for catalyst D which has large pores of 1830 angstroms. The poor reproducibility for catalyst D is believed to come from the rinsing procedure, where a catalyst with large pores is more likely to lose the solution soaked in the peripheral pores than a catalyst with small pores.

Catalysts D and K, with larger pores, show relatively higher values of $D_e$ than catalysts with smaller pores. This is consistent with the model work outlined in the previous paper [1]. The unimodal catalyst C with larger micropores has higher value of $D_e$ compared to the other unimodal catalysts G and I. The small difference in $D_e$ between catalyst G and I may be due to their different pore geometry as evidenced by much different tortuosity values. The bimodal catalyst J, which has only small amount of macropores, shows much smaller $D_e$ values compared to the bimodal catalyst K containing large amount of macropores. The observations agree well, at least qualitatively, with those found in the model work.

$\lambda$ values for each catalyst were calculated based on a critical molecular diameter for octane of 4.9 angstroms [3]. From Eq. (1) the tortuosity, $\tau$, can be expressed as follows:

**Table 5. Results of octane-decane diffusion experiments**

| Catalyst | Size ratio[a] | | $D_i' \times 10^6$ | $D_i \times 10^6$ | $\Sigma\varepsilon_i F_i$ | $\tau$ |
|---|---|---|---|---|---|---|
| | $\lambda_1$ | $\lambda_2$ | $cm^2/s$ | $cm^2/s$ | | |
| G | 0.0891 | n | 3.31± 0.29 | 1.59± 0.14 | 0.392 | 2.78 |
| I | 0.0576 | n | 3.15± 0.27 | 1.73± 0.15 | 0.484 | 3.83 |
| C | 0.0345 | n | 5.35± 0.15 | 2.59± 0.07 | 0.450 | 2.38 |
| D | 0.0098 | 0.0027 | 8.84± 2.21 | 3.77± 0.94 | 0.424 | 1.54 |
| J | 0.0875 | 0.0031 | 4.44± 0.05 | 2.31± 0.03 | 0.437 | 2.59 |
| K | 0.0803 | 0.0021 | 5.00± 0.07 | 3.31± 0.05 | 0.610 | 2.52 |

a: critical molecular diameter of octane = 4.9Å (ref. 10)

n: no macropores

Note: $D_i = \varepsilon_i D_i'$

$\varepsilon_i = \varepsilon K_p = \Sigma\varepsilon_i(1-\lambda_i)^2$(assumed; ref. 10)

$F(\lambda_i) = (1-\lambda_i)^2(1-2.104\lambda_i + 2.09\lambda_i^3 - 0.95\lambda_i^5)$

$\tau = (D_m/D_i)\ \Sigma\varepsilon_i F(\lambda_i)$

$$\tau = (D_m/D_i)\ \Sigma\varepsilon_i F(\lambda_i) \tag{30}$$

where $D_m = 1.37 \times 10^{-5}$ $cm^2/s$ from the Wilke-Chang's relation. The calculation results are listed in the last two columns of Table 5. As expected, catalyst G has the lowest value of $\Sigma\varepsilon_i F(\lambda_i)$. The smallest $\tau$ value observed in catalyst D may come from the fact that the pores of catalyst D are highly likely to be less tortuous because of their large size.

### 3. Polystyrene-Chloroform System

The adsorption of polystyrene was investigated in a manner similar to the octane-decane system. Powdered catalyst K was placed in a bottom-flat flask containing chloroform or polystyrene-chloroform solution. Two polystyrenes of different molecular weights (1,350 and 23,000) were used in this adsorption study. In both the cases the differences in UV readings after a week were ±4%, which indicated that the adsorption term in Eq. (2) was negligible.

The theoretical and experimental polystyrene weights in the diffusion bath at an infinite time are shown in Table 6. Compared to the octane-decane system the deviation between the theoretical and experimental solute weight is a little higher. This may be due to the large size of the polystyrene molecule; i.e. some catalyst pores are smaller than polystyrene; therefore, the pore volume occupied by polystyrene will be a little less than that measured using the water displacement technique. However, the weight deviation does not affect the conclusions drawn in this study.

The effective diffusivity values in the polystyrene-chloroform diffusion system are listed in Table 7. The sizes of polystyrenes were estimated as 12, 19.8, and 27.6 angstroms (Table 3). As typically shown in Fig. 7 the diffusivity data agree well with the theoretical solution curve. In Fig. 7, another set of effective diffusivity data (filled symbol) is presented to show the reproducibility. The effective diffusivity data are reproducible within 0.5 $cm^2/s$.

**Table 6. Comparison of theoretical and experimental solute weight in the bath after a long time in polystyrene-chloroform diffusion experiments**

| Catalyst | Polystyrene sample number | $M_t$, theoretical g | $M_t$, experimental g |
|---|---|---|---|
| G | #50211 | 0.0166 | 0.0134 |
| | #31116 | 0.0240 | 0.0143 |
| C | #31011 | 0.0178 | 0.0162 |
| | #50822 | 0.0171 | 0.0135 |
| | #40717 | 0.0181 | 0.0148 |
| | #50211 | 0.0129 | 0.0124 |
| | #40627 | 0.0165 | 0.0152 |
| | #31116 | 0.0184 | 0.0163 |
| K | #31011 | 0.0395 | 0.0312 |
| | #50822 | 0.0341 | 0.0349 |
| | #40717 | 0.0409 | 0.0387 |
| | #50211 | 0.0440 | 0.0408 |
| | #40627 | 0.0279 | 0.0326 |
| | #31116 | 0.0428 | 0.0402 |
| | #50123 | 0.0386 | 0.0336 |

As expected, the effective diffusivity is strongly dependent upon the ratio of polystyrene to pore size, $\lambda$. For the same catalyst, the effective diffusivity decreases as the polystyrene size increases. When the same molecular weight polystyrene is used, the effective diffusivity decreases in the following catalyst order K>C>G. In other words, the bimodal catalyst K has a higher effective diffusivity than the unimodal

**Table 7. Results of polystyrene-chloroform diffusion experiments**

| Catalyst name | Size ratio[a] $\lambda_1$ | $\lambda_2$ | $D_e' \times 10^7$ cm²/s | $D_e \times 10^7$ cm²/s | $\Sigma\varepsilon_i F_i$ | $\tau$ |
|---|---|---|---|---|---|---|
| G | 0.2182 | n | 10.5± 0.3 | 3.72± 0.20 | 0.1993 | 3.09 |
| | 0.3509 | n | 5.3 | 1.29 | 0.0848 | 2.44 |
| | 0.3927 | n | 3.8 | 0.81 | 0.0623 | 2.59 |
| | 0.4873 | n | 3.1 | 0.47 | 0.0290 | 1.71 |
| C | 0.0845 | n | 21.9 | 9.54 | 0.3589 | 2.17 |
| | 0.0951 | n | 21.0 | 8.94 | 0.3414 | 1.97 |
| | 0.1156 | n | 16.9 | 6.87 | 0.3091 | 2.03 |
| | 0.1359 | n | 12.5 | 4.85 | 0.2793 | 2.15 |
| | 0.1366 | n | 13.4 | 5.19 | 0.2783 | 1.99 |
| | 0.1521 | n | 5.4 | 2.02 | 0.2569 | 4.30 |
| | 0.1887 | n | 5.0 | 1.71 | 0.2111 | 3.43 |
| K | 0.1967 | 0.0051 | 18.1 | 10.7 | 0.4923 | 2.66 |
| | 0.2213 | 0.0057 | 12.8 | 7.35 | 0.4731 | 3.33 |
| | 0.2574 | 0.0067 | 11.1 | 6.15 | 0.4481 | 3.29 |
| | 0.3164 | 0.0082 | 11.3± 0.7 | 5.90± 0.40 | 0.4149 | 2.62 |
| | 0.3180 | 0.0083 | 6.4 | 3.34 | 0.4140 | 4.62 |
| | 0.3541 | 0.0092 | 8.5 | 4.28 | 0.3980 | 3.14 |
| | 0.4393 | 0.0114 | 7.2± 0.3 | 3.35± 0.10 | 0.3703 | 3.08 |

a: The size of polystyrene is shown in Table 3.
n: No macropores
Note: $D_e = \varepsilon_a D_e'$
$\varepsilon_a = \varepsilon K_p = \Sigma\varepsilon_i(1-\lambda_i)^2$
$F(\lambda_i) = (1-\lambda_i)^2(1-2.104\lambda_i + 2.09\lambda_i^3 - 0.95\lambda_i^5)$
$\tau = (D_m/D_e)\ \Sigma\varepsilon_i F(\lambda_i)$

catalysts G and C. Also, the unimodal catalyst C, with the larger pore size, shows higher values in the effective diffusivity than the unimodal catalyst G.

In order to calculate the tortuosity using Eq. (30), the molecular diffusivity was estimated as follows [9]

$$D_m = 1.61 \times 10^{-4}\ M^{-0.525},\ cm^2/s \qquad (31)$$

where M = molecular weight of polystyrene.

The results of tortuosity calculation are shown in the last two columns of Table 7. When compared with the tortuosity obtained in the octane-decane system, the tortuosity in the polystyrene-chloroform is much more dependent upon $\lambda$. This result indicates that the tortuosity is not a constant but a function of $\lambda$. A similar observation has been reported in the literature [2, 10]. Smith [2] developed a simple model showing that the tortuosity is dependent on $\lambda$. However, the dependence of tortuosity on $\lambda$ cannot be predicted a priori for a specific porous catalyst. He also argued that the discrepancies in the experimental and theoretical effective diffusivity mainly resulted from assuming a constant tortuosity. His argument can be extended to explain the tortuosity data listed in Table 7.

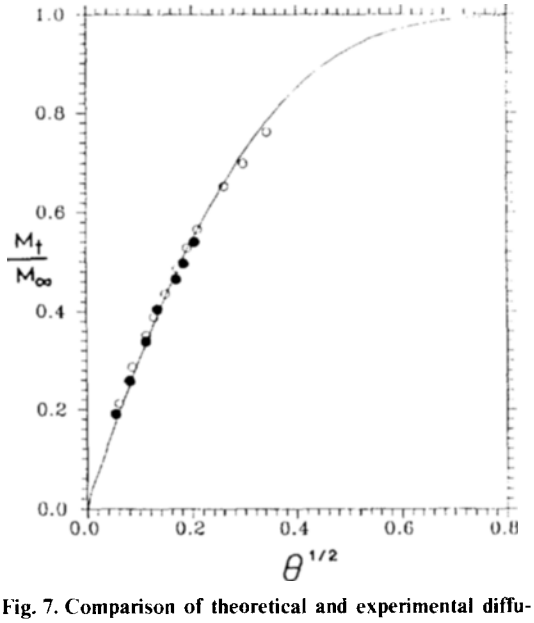


**Fig. 7. Comparison of theoretical and experimental diffusion data for catalyst K in polystyrene # 50123-chloroform system.**

**Table 8. Effects of λ on H(λ) in unimodal catalysts**

| Diffusion system | Catalyst | λ | H(λ) |
|---|---|---|---|
| Octane-decane | G | 0.0891 | 0.241 |
| | I | 0.0576 | 0.230 |
| | C | 0.0345 | 0.390 |
| Polystyrene-chloroform | G | 0.2182 | 0.182 |
| | | 0.3509 | 0.142 |
| | | 0.3927 | 0.113 |
| | | 0.4873 | 0.111 |
| | C | 0.0845 | 0.380 |
| | | 0.0951 | 0.407 |
| | | 0.1156 | 0.375 |
| | | 0.1359 | 0.335 |
| | | 0.1366 | 0.360 |
| | | 0.1521 | 0.160 |
| | | 0.1887 | 0.180 |

Note: $H(\lambda)=D_i/(\varepsilon_{ii}D_m)=D_i'/D_m$

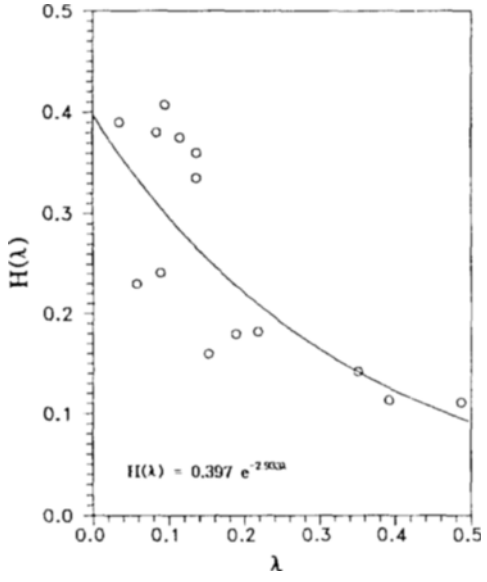


**Fig. 8. Effect of λ on H(λ) in both octane-decane and polystyrene-chloroform diffusion systems.**

Apparently, the steric exclusion-hydrodynamic drag theory, used in calculating the tortuosity, does not explain the variation in the tortuosity shown in Table 7.

Thus, Eq. (1) can be rewritten as follows:

$$\begin{aligned} D_i &= D_m\Sigma\varepsilon_i F(\lambda_i)/\tau \\ &= D_m\Sigma(\varepsilon_i K_{pi})K_{ri}/\tau \\ &= D_m\Sigma(\varepsilon_{ii})_i H(\lambda_i) \end{aligned} \tag{32}$$

In Eq. (32), H(λ) can be determined from the effective diffusivity, $D_i$, molecular diffusivity, $D_m$, and available porosity, $\varepsilon_{ii}$. To make matters simple, H(λ) was calculated using the data of unimodal catalysts and then its applicability to bimodal catalysts was evaluated. The calculated values of H(λ) are listed in Table 8.

In order to derive an empirical equation relating λ to H(λ), an exponential curve fitting was attempted as shown in Fig. 8. Similar approaches are available in the literature [10, 11]. In Fig. 8, the H(λ) data of both polystyrene-chloroform and octane-decane systems are plotted. A best least squares fit gives the following empirical equation.

$$H(\lambda)=0.397\ e^{-2.933\lambda} \tag{33}$$

This equation was evaluated using the data for bimodal catalysts.

For bimodal catalysts,

$$\begin{aligned} H(\lambda) &= D_i'/D_m \\ &= D_i/(\varepsilon_{ii}D_m) \\ &= [\Sigma(\varepsilon_{ii})_i H(\lambda_i)]/\varepsilon_{ii} \\ &= [\Sigma\varepsilon_i(1-\lambda_i)^2 H(\lambda_i)]/[\Sigma\varepsilon_i(1-\lambda_i)^2] \end{aligned} \tag{34}$$

The evaluation result of Eq. (33) is listed in Table 9. The H(λ) values predicted using the empirical equations show good agreement with those obtained experimentally for all bimodal catalysts except catalyst D. The extremely large deviation for catalyst D obviously comes from the poor reproducibility of measuring its effective diffusivity. When the data of catalyst D are excluded, Eq. (33) shows a standard deviation of 0.052.

In Eq. (33) the pre-exponential constant is reciprocal of the tortuosity value at $\lambda=0$. In other words, $\tau_{ii}=1/H(0)=2.52$, which is physically plausible. The tortuosity values for catalysts G, C, and K are close to this value as shown in the octane-decane system where λ can

**Table 9. Evaluation of H(λ) in bimodal catalysts**

| Diffusion system | Catalyst | H(λ) | |
|---|---|---|---|
| | | Experimental | Predicted |
| Octane-decane | D | 0.645 | 0.393 |
| | J | 0.324 | 0.319 |
| | K | 0.365 | 0.357 |
| Polystyrene-chloroform | K | 0.314 | 0.325 |
| | | 0.248 | 0.321 |
| | | 0.246 | 0.317 |
| | | 0.303 | 0.313 |
| | | 0.252 | 0.313 |
| | | 0.259 | 0.317 |

Note: $H(\lambda)=D_i'/D_m$
$=[\Sigma\varepsilon_i(1-\lambda_i)^2H(\lambda_i)]/[\Sigma\varepsilon_i(1-\lambda_i)^2]$

be practically considered as zero.

Eq. (33) is compared to empirical equations reported in the literature [2, 11, 12]. Satterfield et al. [11] derived a similar equation on the basis of diffusion experiments involving various molecules in silica-alumina beads. Also, Chantong and Massoth [12] reported a similar equation obtained from the diffusion experiment with polyaromatic compounds in aluminas.

Eq. (33) is much different from the expression of the restrictive factor shown in the previous paper [1]. Thus, this equation can be effectively used to predict the effective diffusivity when $\lambda$, $\varepsilon_a$, and $D_m$ are known.

## CONCLUSION

The experimental diffusivity data agreed well with the theoretical solution curve. The catalysts with larger micropores or large amount of macropores showed higher effective diffusivities as predicted by the simplified model developed in the previous work.

When the steric exclusion-hydrodynamic drag theory was applied, the tortuosity was found to be a function of the ratio of diffusing molecule to catalyst pore size. An empirical equation correlating the size ratio, $\lambda$, to the restrictive factor, $F(\lambda)$, was obtained. This equation fitted the diffusivity data of bimodal catalysts within 7% deviation.

## ACKNOWLEDGMENT

The authors thank the U.S. Department of energy for the financial support of this study through the Consortium for Fossil Fuel Liquefaction Science.

## NOMENCLATURE

- $C$ : solute concentration based on total pore volume [mole/$l$]
- $C_b$ : solute concentration in the bulk fluid [mole/$l$]
- $d$ : pellet diameter [cm]
- $D_e$ : effective diffusivity [cm$^2$/s]
- $D_e'$ : $D_e/\varepsilon_a$ [cm$^2$/s]
- $D_m$ : molecular bulk diffusivity [cm$^2$/s]
- $F(\lambda)$ : combined function of $K_r$ and $K_p$
- $H(\lambda)$ : restrictive factor
- $J$ : Bessell function
- $K_p$ : steric coefficient
- $K_r$ : frictional drag coefficient
- $l$ : number of data in Fig. 4
- M's : molecular weight in Table 3
- $M_t$ : total amount of the solute diffusing out of the pellets till time t [mg]
- $M_\infty$ : $M_t$ at time $=\infty$
- $n$ : unit vector; constant
- $N_A$ : flux of component A [mole/cm$^2$-s]
- $q$ : amount of adsorption by solute onto pellet [mole/g of pellet]
- $r$ : radial distance in cylindrical pellet [cm]
- $R$ : size of polystyrene defined in Table 3
- $S$ : specific surface area [m$^2$/g]
- $t$ : time [s]
- $T$ : temperature [°K]
- $V_b$ : bulk volume [cc]
- $V_{pm}$ : available pore volume [cc]
- $V_p$ : total pellet volume [cc]
- $X_n$ : roots in Eq. (27)
- $Y_n$ : roots in Eq. (27)

### Greek Letters

- $\alpha$ : volume ratio defined in Eq. (22)
- $\beta$ : root in the Bessel function
- $\varepsilon$ : porosity
- $\varepsilon_a$ : available volume porosity
- $\lambda$ : ratio of molecule radius to pore radius
- $\rho_p$ : pellet density (apparent density) [g/cc]
- $\sigma$ : standard deviation
- $\tau$ : tortuosity
- $\theta$ : dimensionless time defined in Eq. (13)
- $\xi$ : dimensionless variable defined in Eq. (14)

### Superscript

- * : for dimensionless variables

### Subscripts

- 1 : for micropores; for slab geometry
- 2 : for macropores; for cylindrical geometry
- i : for initial condition at t=0
- o : for initial values at t=0
- t : for time t or for total
- $\infty$ : for an infinite time

## REFERENCES

1. Rhee, Y. W. and Guin, J. A.: *KJChE*, **10**, 56 (1993).
2. Seo, G. and Massoth, F. E.: *AIChE J.*, **31**, 494 (1985).
3. Tsai, K. J.: Ph.D. Thesis, Auburn University, Auburn, AL (1985).
4. Prasher, B. D. and Ma, Y. H.: *AIChE J.*, **23**, 303 (1977).
5. Holman, J. P.: "Heat Transfer", 6th ed., p. 155, McGraw-Hill Book Company, New York, 1986.
6. Crank, J.: "The Mathematics of Diffusion", 2nd ed., p. 48 & 73, Oxford University Press, London,

1975.
7. Abramowitz, M. and Stegun, I. A.: "Handbook of Mathematical Functions", p. 409, Dover Publications, Inc., New York, 1965.
8. Crank, J.: "The Mathematics of Diffusion", 2nd ed., p. 57 & 77. Oxford University Press, London, 1975.
9. Colton, C. K., Satterfield, C. N. and Lai, C. J.: *AIChE J.*, **21**, 289 (1975).
10. Smith, D. M.: *AIChE J.*, **32**, 1039 (1986).
11. Satterfield, C. N., Colton, C. K. and Pitcher, W. H.: *AIChE J.*, **19**, 628 (1973).
12. Chantong, A. and Massoth, F. E.: *AIChE J.*, **29**, 725 (1983).